



# Chapter VI: Cool supergiants



# Variable mass loss on 100 yr timescales from massive yellow hypergiants

René D. Oudmaijer<sup>1</sup>  and Evgenia Koumpia<sup>2</sup>

<sup>1</sup>School of Physics & Astronomy, University of Leeds, Woodhouse Lane, LS2 9JT Leeds, UK  
email: [R.D.Oudmaijer@leeds.ac.uk](mailto:R.D.Oudmaijer@leeds.ac.uk)

<sup>2</sup>ESO Vitacura, Alonso de Córdova 3107 Vitacura, Casilla 19001 Santiago de Chile, Chile

**Abstract.** This contribution presents new results on two members of the class of post-Red Supergiants, IRAS 17163-3907, the central star of the Fried Egg nebula and IRC +10420. New optical spectra in the blue spectral range confirm their spectral type to be of A-supergiant class. Our VLTI/GRAVITY *K*-band interferometry reveals that the neutral Na I 2.2  $\mu\text{m}$  line emitting region is smaller than that of the hydrogen Br $\gamma$  emission. This can be explained with the hydrogen emission the result of collisional excitation populating the higher levels in a neutral region instead them being populated through recombination in an ionised environment as mostly inferred in stellar winds. Finally, the central star of the Fried Egg nebula, has undergone 3 distinct mass loss episodes over the last hundreds of years. As it is likely that at least the last mass loss event occurred when the star was already a Yellow Hypergiant and not a Red Supergiant, we put forward the bi-stability mechanism as explanation for the mass loss.

**Keywords.** stars: evolution, stars: mass-loss, stars: AGB and post-AGB, stars: individual: IRAS 17163-3907; IRC+10420, circumstellar matter

---

## 1. Introduction

The post-Red Supergiant (post-RSG) stars are evolved massive stars that are moving to the left in the HR diagram. Although occupying similar locations in the HR diagram, they are different from the Yellow Hypergiants (YHG) by having massive dust shells betraying a previous mass losing phase which has been identified with the RSG stage. At present their ultimate fate is not overly clear. They may evolve to higher temperatures to become Luminous Blue Variables, B[e] supergiants or Wolf-Rayet stars, or even “bounce back” from what has been coined to be the Yellow Void or White Wall and move back to cooler temperatures (see reviews by [de Jager 1998](#); [Oudmaijer et al. 2009](#); [Gordon and Humphreys 2019](#)). Not many such objects are known, and in this contribution we highlight our recent work on the objects IRAS 17163-3907 and IRC +10420 presented in [Koumpia et al. \(2020\)](#) and [Koumpia et al. \(2022\)](#) respectively. IRC +10420 had been known for a long time to be a massive evolved object ([Humphreys et al. 1973](#); [Jones et al. 1993](#); [Oudmaijer et al. 1996](#)), while despite its IR brightness, IRAS 17163-3907 (or Hen 3-1379), the central star of the Fried Egg Nebula was only recognised relatively late to be of massive nature ([Lagadec et al. 2011](#)). Below we will focus on the optical spectroscopy and near-infrared spectro-interferometry we have obtained.

## 2. Stellar Temperatures

The optical spectra of both objects are swamped with emission lines in the red part of the spectrum. [Wallström et al. \(2015\)](#) compared the emission line spectra of both objects

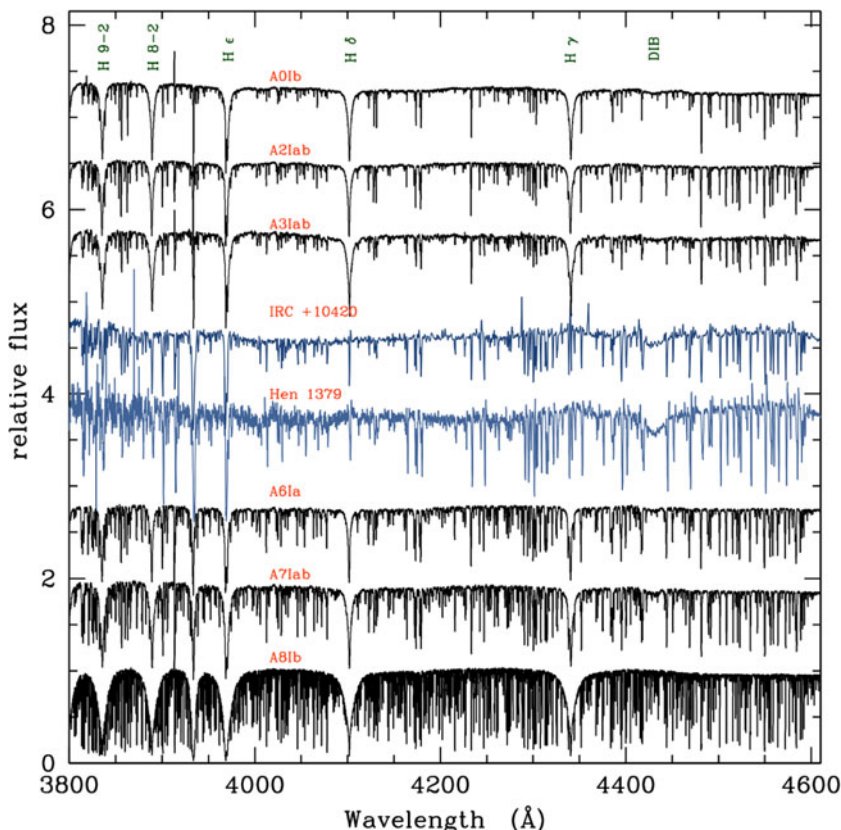


**Figure 1.** Blue optical spectra of Hen 3-1379 and IRC+10420 obtained with X-Shooter and as presented in Koumpia et al. (2020) and Koumpia et al. (2022) respectively. Data have been rebinned to improve the signal-to-noise, are continuum normalised and offset by increases of 1. For reference spectra of spectral standard stars from Bagnulo et al. (2003) are plotted. Both objects have a spectrum consistent with a mid-A supergiant spectral type.

and find a striking similarity. Given the relative faintness and red colours of the objects, not many blue spectra have been published. It is in this spectral region that the emission lines are less prominent or absent, allowing spectral typing to be done. For IRC +10420, using the only blue spectrum published up until Koumpia et al. (2022), Oudmaijer (1998) was able to assign an A-supergiant type, while, based on the same data, in a dedicated study Klochkova et al. (1997) computed a temperature of 8500 K. For the Fried Egg, Koumpia et al. (2020) determined a similar spectral type based on the only blue spectrum so far. In Fig. 1 we show X-Shooter data of both objects and compare them with those of several spectral standard stars. The spectra of both objects are similar and can be assigned a similar spectral class. The IRC +10420 spectrum was obtained in 2009, and is presented in Koumpia et al. (2022). It does not show any significant variations with respect to its spectrum taken 15 years earlier, signifying that its earlier observed rapid increase in temperature (2000 K in 20 years - Oudmaijer 1998) has halted.

### 3. VLTI/GRAVITY data around Br $\gamma$ and Na I

We observed both objects with near-infrared interferometry in the *K*-band spectral region using VLTI/GRAVITY. In Fig. 2, we show the spectrum as well as their visibilities at the longest baseline ( $\sim 120$  m). To recap, a visibility of 1 would indicate an

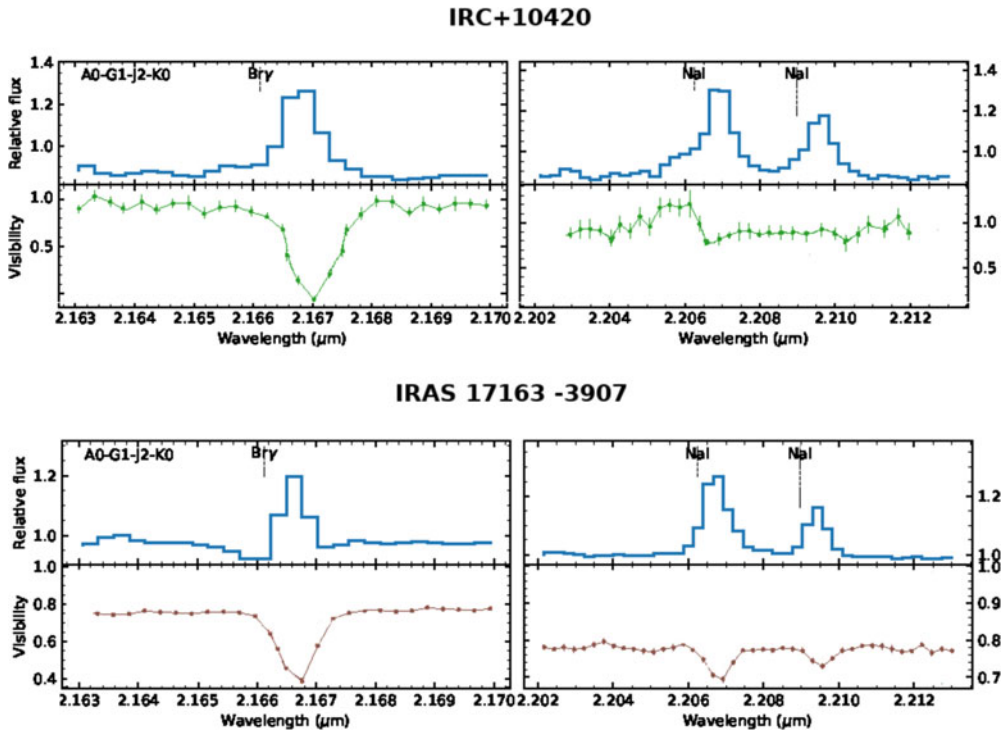


**Figure 2.** The GRAVITY spectra and visibilities at the longest baselines ( $\sim 120$  m) which are sensitive to the smallest scales for the IRC+10420 (top) and Fried Egg (bottom). Note that in both cases the central source is barely resolved and is identified with the star, while the Na I doublet at  $2.2 \mu\text{m}$  appears to come from a smaller emitting regions than  $\text{Br}\gamma$  at  $2.16 \mu\text{m}$ .

unresolved point source (roughly 2 milli-arcsec in the present data) within the field-of-view of the interferometer, while the lower the visibility, the more extended the source is. In both cases, the continuum appears unresolved and traces the stellar continuum, while also in both cases, the Na I emission region is smaller than that of the hydrogen emission. It may be interesting to note that although rare, Na I  $2.2 \mu\text{m}$  doublet emission appears to be present in the spectrum of many YHGs (IRC+10420, HD 179821, HR 8752, and  $\rho$  Cas (Lambert et al. 1981; Hrivnak et al. 1994; Hanson et al. 1996; Oudmaijer and de Wit 2013). Various explanations for the origin of the Na I  $2.2 \mu\text{m}$  doublet emission are discussed in literature (for an overview see e.g. Oudmaijer and de Wit 2013), the spatial information here helps us to constrain the various models.

We would like to draw attention to the fact that the neutral sodium's emission region is smaller than that of the hydrogen,  $\text{Br}\gamma$ , emission. The puzzling issue here is that we have very strong hydrogen emission from a relatively cool star, while in addition, neutral sodium originates from inside the hydrogen emitting region. The latter is counter-intuitive, generally it is assumed that hydrogen emission is due to recombination. This of course implies that the hydrogen has to be ionised to begin with, yet the ionisation potential of sodium is much lower than that of hydrogen (5.1 eV versus 13.6 eV). So the question arises why Na would be neutral while it is located closer to the star than the ionised hydrogen.

A solution could be that the hydrogen emission is not due to recombination, but due to collisional excitation; in regions of high density, collisions can excite electrons to higher energy levels, while their de-excitation can give rise to line emission without the need

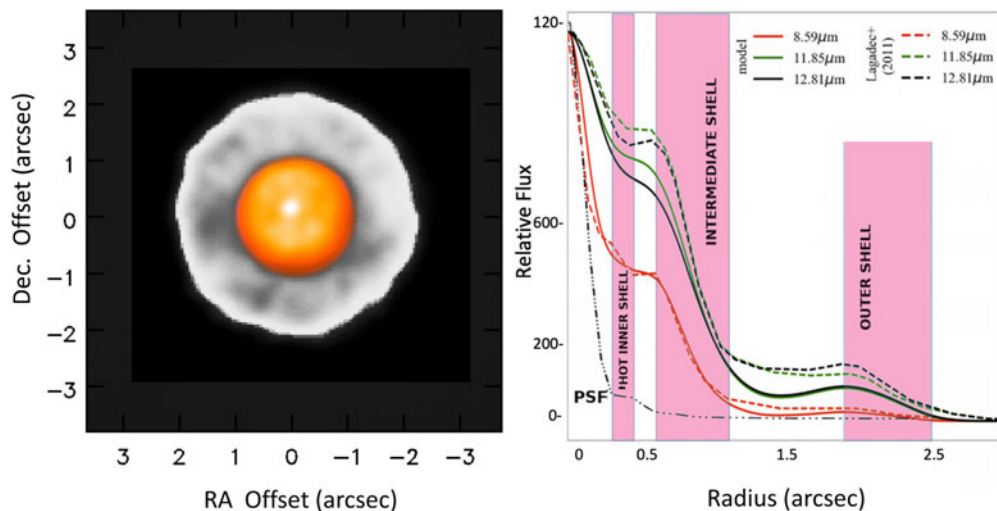


**Figure 3.** Left:  $10\ \mu\text{m}$  VISIR image of the Fried Egg nebula adapted from Lagadec et al. (2011). The presence of two separate shells is readily visible. Right: the radial profile reveals the presence of 3 resolved shells.

for ionisation, and thus occur in a neutral region. We explored this notion using simple LTE models and are able to explain the  $2\ \mu\text{m}$  observations of the Fried Egg for the size scales and emission line strengths (Koumpia et al. 2020). The next step is to approach this with kinematic modelling and ultimately to arrive at a description of the immediate circumstellar environment of the stars.

#### 4. Variable mass loss

The  $10\ \mu\text{m}$  diffraction limited images that led Lagadec et al. (2011) to introduce the name “Fried Egg” (see Fig. 3) already reveals a discontinuity in the dust density distribution. In fact, the radial profile of the emission (also in the Figure) reveals the presence of 3 distinct shells, which all have kinematic ages less than hundreds of years. The simultaneous modelling of the object’s spectral energy distribution and the spatial information, revealed that these shells can be understood in terms of short periods of enhanced mass loss (Koumpia et al. 2020). These mass loss periods were preceded by a much earlier period of mass loss which is traced on larger scales by Herschel observations at longer wavelengths (Hutsemékers et al. 2013).

An outstanding question is what could lead to these short bursts of mass loss. Traditionally, in the case of Yellow Hypergiants, pulsational instabilities have been proposed to do so (e.g. Lobel et al. 1994), however not much is known about any photometric or spectroscopic variability of the central star of the Fried Egg nebula that could reveal information about its pulsational properties. Instead, it could be argued that the object has remained fairly stable in its spectral appearance and photometry since Lebertre et al. (1989). As the innermost shell has a kinematic age that is comparable to the time that has lapsed since Lebertre et al. (1989)’s observations, it is reasonable to assume it was ejected when the star was of A-spectral type.

This inference led us to consider an alternative mass loss mechanism which is due to the so-called “bi-stability jump”. This mechanism is known to occur around 20,000 K. At this temperature, the ionisation stage of iron changes from Fe IV to Fe III. The line opacity of iron far exceeds that of the more abundant H and He, and is the main contribution to the opacity responsible for driving winds of hotter stars. As the opacity depends on the

ionisation levels, any change in temperature around this ionisation boundary will result in different wind properties. For example, a slight decrease in temperature across the “bi-stability” jump, will lead to recombination of Fe, leading to a larger wind density and smaller wind velocities by a factor of 2. This has been well-studied for the “first” bi-stability jump at  $T \sim 20,000$  K, however, a “second” bi-stability jump, which thus far has not received much attention, is expected to occur at  $T \sim 8800$  K.

The A-supergiants under consideration here straddle the temperature range of the second bi-stability jump (the temperature at which the dominant ionisation stage of iron changes from triply to doubly ionised, Vink et al. 2000, 2001; Petrov et al. 2016). Koumpia et al. (2020) pointed out that a similar change in mass loss could arise as for the, much better known, first bi-stability jump (Vink et al. 1999) that occurs at temperatures of order 20,000 K.

As even slight changes in temperature can lead to comparatively large changes in mass loss rates in the Yellow Hypergiant spectral type range, the observations of very recent mass loss episodes for the central star of the Fried Egg nebula means that this relatively unexplored “second” bi-stability jump warrants further study.

## 5. Concluding remarks

New spectral and near-infrared interferometric data on key post-Red Supergiants allowed us to reach several conclusions:

- The optical spectra of both the central star of the Fried Egg nebula and IRC +10420 are remarkably similar in both their emission line spectrum in the red, as are their absorption line spectra in the blue spectral range. Both have spectral types corresponding to A-type supergiants. IRC +10420 appears not to have changed its spectral type since 1994 signifying it has halted its previously observed blueward evolution in the HR diagram.

- The VLTI/GRAVITY *K*-band interferometry reveal an unresolved continuum for both stars which we identify with the stellar photospheres. Any extended *K*-band emission due to thermal emission from dust falls outside the interferometer’s field-of-view. The neutral Na I at 2.2  $\mu\text{m}$  line emitting region is smaller than that of the hydrogen Br $\gamma$  emission. This can be explained with the hydrogen emission being due to collisional excitation populating the higher levels, followed by de-excitations instead of the usually assumed recombination in an ionised gas. Simple LTE model approaches can reproduce the line strengths and the respective size scales.

- Hen 3-1379, the central star of the Fried Egg nebula, has undergone 3 distinct mass loss episodes over the last hundreds of years. As it is likely that at least the last mass loss event occurred when the star was already a Yellow Hypergiant and not a Red Supergiant, we put forward the bi-stability mechanism as explanation for the mass loss.

## Acknowledgements

EK was funded by the STFC (ST/P00041X/1) This project has received funding from the European Union’s Framework Programme for Research and Innovation Horizon 2020 (2014-2020) under the Marie Skłodowska-Curie Grant Agreement No. 823734.

## References

- Bagnulo, S., Jehin, E., Ledoux, C., Cabanac, R., Melo, C., Gilmozzi, R., & ESO Paranal Science Operations Team 2003, The UVES Paranal Observatory Project: A Library of High- Resolution Spectra of Stars across the Hertzsprung-Russell Diagram. *The Messenger*, 114, 10–14.
- de Jager, C. 1998, The yellow hypergiants. *A&A Rev.*, 8(3), 145–180.
- Gordon, M. S. & Humphreys, R. M. 2019, Red Supergiants, Yellow Hypergiants, and Post-RSG Evolution. *Galaxies*, 7(4), 92.

- Hanson, M. M., Conti, P. S., & Rieke, M. J. 1996, A Spectral Atlas of Hot, Luminous Stars at 2 Microns. *ApJS*, 107, 281.
- Hrivnak, B. J., Kwok, S., & Geballe, T. R. 1994, Near-infrared spectroscopy of proto-planetary nebulae. *ApJ*, 420, 783–796.
- Humphreys, R. M., Strecker, D. W., Murdock, T. L., & Low, F. J. 1973, IRC+10420 - Another Eta Carinae? *ApJL*, 179, L49.
- Hutsemékers, D., Cox, N. L. J., & Vamvatira-Nakou, C. 2013, A massive parsec-scale dust ring nebula around the yellow hypergiant Hen 3-1379. *A&A*, 552, L6.
- Jones, T. J., Humphreys, R. M., Gehrz, R. D., Lawrence, G. F., Zickgraf, F.-J., Moseley, H., Casey, S., Glaccum, W. J., Koch, C. J., Pina, R., Jones, B., Venn, K., Stahl, O., & Starrfield, S. G. 1993, IRC +10420: A Cool Hypergiant near the Top of the HRD. *ApJ*, 411, 323.
- Klochkova, V. G., Chentsov, E. L., & Panchuk, V. E. 1997, Optical spectrum of the IR source IRC+10420 in 1992-1996. *MNRAS*, 292, 19.
- Koumpia, E., Oudmaijer, R. D., de Wit, W. J., Mérand, A., Black, J. H., & Ababakr, K. M. 2022, Tracing a decade of activity towards a yellow hypergiant. The spectral and spatial morphology of IRC+10420 at au scales. *MNRAS* in press., arXiv:2207.05812.
- Koumpia, E., Oudmaijer, R. D., Graham, V., Banyard, G., Black, J. H., Wichittanakom, C., Ababakr, K. M., de Wit, W. J., Millour, F., Lagadec, E., Muller, S., Cox, N. L. J., Zijlstra, A., van Winckel, H., Hillen, M., Szczerba, R., Vink, J. S., & Wallström, S. H. J. 2020, Optical and near-infrared observations of the Fried Egg Nebula. Multiple shell ejections on a 100 yr timescale from a massive yellow hypergiant. *A&A*, 635, A183.
- Lagadec, E., Zijlstra, A. A., Oudmaijer, R. D., Verhoelst, T., Cox, N. L. J., Szczerba, R., Mékarnia, D., & van Winckel, H. 2011, A double detached shell around a post-red supergiant: IRAS 17163-3907, the Fried Egg nebula. *A&A*, 534, L10.
- Lambert, D. L., Hinkle, K. H., & Hall, D. N. B. 1981, Circumstellar shells of luminous supergiants. I - Carbon monoxide in Rho Cassiopeiae and HR 8752. *ApJ*, 248, 638–650.
- Lebertre, T., Epchtein, N., Gouiffes, C., Heydari-Malayeri, M., & Perrier, C. 1989, Optical and infrared observations of four suspected proto-planetary objects. *A&A*, 225, 417–431.
- Lobel, A., de Jager, C., Nieuwenhuijzen, H., Smolinski, J., & Gesicki, K. 1994, Pulsation of the yellow hypergiant  $\rho$  Cassiopeiae in 1970. *A&A*, 291, 226–238.
- Oudmaijer, R. D. 1998, High resolution spectroscopy of the post-red supergiant IRC+10420. I. The data. *A&AS*, 129, 541–552.
- Oudmaijer, R. D., Davies, B., de Wit, W.-J., & Patel, M. Post-Red Supergiants. In Luttermoser, D. G., Smith, B. J., & Stencel, R. E., editors, *The Biggest, Baddest, Coolest Stars 2009*, volume 412 of *Astronomical Society of the Pacific Conference Series*, 17.
- Oudmaijer, R. D. & de Wit, W. J. 2013, Neutral and ionised gas around the post-red supergiant IRC +10 420 at AU size scales. *A&A*, 551, A69.
- Oudmaijer, R. D., Groenewegen, M. A. T., Matthews, H. E., Blommaert, J. A. D. L., & Sahu, K. C. 1996, The spectral energy distribution and mass-loss history of IRC+10420. *MNRAS*, 280, 1062–1070.
- Petrov, B., Vink, J. S., & Gräfener, G. 2016, Two bi-stability jumps in theoretical wind models for massive stars and the implications for luminous blue variable supernovae. *MNRAS*, 458(2), 1999–2011.
- Vink, J. S., de Koter, A., & Lamers, H. J. G. L. M. 1999, On the nature of the bi-stability jump in the winds of early-type supergiants. *A&A*, 350, 181–196.
- Vink, J. S., de Koter, A., & Lamers, H. J. G. L. M. 2000, New theoretical mass-loss rates of O and B stars. *A&A*, 362, 295–309.
- Vink, J. S., de Koter, A., & Lamers, H. J. G. L. M. 2001, Mass-loss predictions for O and B stars as a function of metallicity. *A&A*, 369, 574–588.
- Wallström, S. H. J., Muller, S., Lagadec, E., Black, J. H., Oudmaijer, R. D., Justtanont, K., van Winckel, H., & Zijlstra, A. A. 2015, Investigating the nature of the Fried Egg nebula. CO mm-line and optical spectroscopy of IRAS 17163-3907. *A&A*, 574, A139.



## Discussion

JESÚS MAÍZ APPELÁNIZ: I checked Gaia EDR3 and find that the distance to IRAS 17163-3907 is 5 kpc, but with a large errorbar.

RENÉ OUDMAIJER: It is indeed. The pre-Gaia distance to the object was mainly based on the kinematic distance of both object and interstellar absorption lines and the large interstellar extinction value. This led to a distance of 1 kpc, which happens to be consistent with the Gaia DR2 distance. 1 kpc already results in a luminosity that is half a million times solar, so 5 kpc would really give an extremely large value for the brightness.

SALLY OEY: Do you have kinematic info on the Br $\gamma$  and Na I?

RENÉ OUDMAIJER: Yes, however, Br $\gamma$  might be affected by possible P Cygni absorption. We have LSR velocities for Na (25 km/s), CO mm (18 km/s), H30 $\alpha$  (21 km/s) and interstellar KI (-32, -10, 6), many pointing at large distances indeed.

SALLY OEY: Thanks, was wondering whether there was an offset between them, but apparently not interesting.

ALEXIS QUINTANA: Following Maíz Appelániz' question, I remember that Bailer-Jones's last catalogue gives two distances typically, including photogeometric distances. If I remember correctly these set of distances take extinction into account. Since this object has a very high extinction ( $A_V = 11$  mag), could the photogeometric distance be more reliable, or are the uncertainties too high as well?

RENÉ OUDMAIJER: That is a good point - however the distances that take into account reddening etc may work well for the 99.999% of normal stars in the Galaxy, but I have learned the hard way that they do not work well for objects that are a-typical. It will be interesting to see how DR3 and later will deal with such objects.